Clim. Past Discuss., 5, 1989–2018, 2009
www.clim-past-discuss.net/5/1989/2009/

Climate of the Past Discussions

Climate of the Past Discussions is the access reviewed discussion forum of *Climate of the Past*

Anomalously high Arabian Sea productivity conditions during MIS 13

M. Ziegler[1], L. J. Lourens[1], E. Tuenter[2], and G.-J. Reichart[1]

[1]Department of Earth Sciences, Utrecht University, Utrecht, The Netherlands
[2]Institute for Marine and Atmospheric research Utrecht (IMAU), Utrecht University, Utrecht, The Netherlands

Received: 14 July 2009 – Accepted: 15 July 2009 – Published: 27 July 2009

Correspondence to: M. Ziegler (ziegler@geo.uu.nl)

Published by Copernicus Publications on behalf of the European Geosciences Union.

Abstract

Marine isotope stage (MIS) 13 (∼500 000 years ago) has been recognized as atypical in many paleoclimate records and, in particular, it has been connected to an exceptionally strong summer monsoon in East Asia. Here we present a multi-proxy study of a sediment core taken from the Murray Ridge at intermediate water depth in the northern Arabian Sea that covers the last 750 000 years. Our results indicate that upwelling driven primary productivity conditions were anomalously high during MIS 13 and led to extreme carbonate dissolution and glauconitization. We argue that an extreme summer monsoon circulation was probably not responsible for these aberrant conditions, because such an event does not show up in the Antarctic methane record and transient modeling results. As an alternative, we propose that high productivity was related to the onset of an intensive meridional overturning circulation in the Atlantic Ocean at the end of the Mid-Pleistocene transition. This led to an increased supply of nutrient-rich deep waters into the Indian Ocean euphotic zone, thereby triggering the observed productivity maximum.

1 Introduction

The Mid-Pleistocene transition (MPT) characterizes a fundamental change in the climate state which allowed ice sheets to expand and evolve from a dominant 41 ka (obliquity) to a quasi ∼100 ka rhythm (Clark et al., 2006; Lisiecki and Raymo, 2005; Raymo and Nisancioglu, 2003; Raymo et al., 2006; Shackleton and Opdyke, 1976). The end of the MPT between ca. 600 and 500 ka is described by a series of events (Schmieder et al., 2000). First, the transition between MIS 14 and 13 (i.e., termination TVI) is the least pronounced termination of the past 640 ka. Ice volume has increased only minor during MIS 14 as compared to the other late Pleistocene glacial periods. A record from Lake Baikal indicates for instance that mountain glaciations were reduced in central Eurasia from 580 to 380 ka ago (Prokopenko et al., 2002). In particular, the record

CPD

5, 1989–2018, 2009

documents a continuous forestation, suggesting that mild winter conditions prevailed with relatively little snow cover.

MIS 13 is on the other hand exceptional. It marks an extreme $\delta^{13}C_{max}$ associated with a major reorganization in the carbon reservoir of the global ocean (Wang et al., 2003). Several peculiarities occur in the ocean during this time, such as thick laminated layers of the giant diatom *Ethmodiscus rex* in the Atlantic Ocean (Romero and Schmieder, 2006). Also the climate changed dramatically during this period with high terrigenous influx at Ceara Rise (Harris et al., 1997), indicating heavy precipitation in the Amazon Basin, or the exceptional thick soil horizon S5 found at the Chinese loess plateau (CLP) (Guo et al., 2009; Sun et al., 2006b). Moreover, extreme Indian monsoon intensity inferred from the occurrence of the anomalous sapropel Sa in the Mediterranean and a peak in planktic oxygen isotope records from the equatorial Indian Ocean (Bassinot et al., 1994; Rossignol-Strick et al., 1998) is commonly linked to this event (Guo et al., 2009; Yin and Guo, 2008). However, both events occurred during MIS 14 and have therefore potentially a different origin.

The transition between MIS 14 and 13 coincides furthermore with the onset of the Mid-Brunhes dissolution interval (MBDI), which lasts until ~280 ka (Barker et al., 2006; Bassinot et al., 1994; Droxler et al., 1988). This period of extensive dissolution in the deep sea is probably not caused by enhanced greenhouse forcing, since Antarctic ice core data and boron isotopes indicate generally low atmospheric $p\mathrm{CO_2}$ levels even within interglacial periods during this time (Hönisch et al., 2009; Petit, 1999). An alternative explanation for the MBDI invokes an increase in low-latitude shelf carbonate production (Droxler et al., 1997). In extension to that, it has been suggested that pelagic carbonate production increased globally, due to the proliferation of the coccolithophore *Gephyrocapsa* (Bollmann et al., 1998), thereby causing widespread dissolution in the deep sea (Barker et al., 2006). Most severe dissolution occurs during MIS 11, which follows on the so-called Mid-Brunhes event at ca 430 ka (i.e., termination TV), representing the largest-amplitude change in $\delta^{18}O$ of the global ocean over the past 6 m y (Wang et al., 2003).

In 2004, a long sediment core was drilled at the Murray Ridge, a submarine high in the northeastern Arabian Sea, from a water depth of 2387 m well below the present-day extension of the oxygen minimum zone (OMZ). The main aim of retrieving this core was to investigate the paleoceanographic changes in the Arabian Sea during the MPT, since numerous studies document these only in great detail of the past 400 000 years (Almogi-Labin et al., 2000; Altabet et al., 2002; Anderson et al., 2002; Budziak et al., 2000; Clemens et al., 1991; Clemens and Prell, 1990, 2003; Emeis et al., 1995; Gupta et al., 2003; Ishikawa and Motoyoshi, 2007; Ivanova et al., 2003; Jaeschke et al., 2009; Leuschner and Sirocko, 2000, 2003; Lückge et al., 2001; Naidu and Malmgren, 1996; Naidu, 2006; Pattan et al., 2003; Prabhu and Shankar, 2005; Prell et al., 1980; Prell and Campo, 1986; Prell and Kutzbach, 1992; Reichart et al., 1997; Reichart et al., 1998; Reichart et al., 2002; Reichart et al., 2004; Rostek et al., 1993; Rostek et al., 1997; Saher et al., 2007; Sarkar et al., 1990; Schmiedl and Leuschner, 2005; Schulte et al., 1999; Schulz et al., 1998; Sirocko et al., 1993; Sirocko et al., 1996; Wang et al., 2005a). Using a multi-proxy approach we will report on the complex interplay of summer monsoon upwelling-related productivity changes, OMZ intensity, glacial-interglacial variability in intermediate water contributions, supralysoclinal carbonate dissolution and winter monsoon-related deep-mixing events. Special emphasis will be on the cause of the exceptional high productivity conditions in the Arabian Sea during MIS 13.

2 Material and methods

2.1 Sediment core MD04-2881

The sedimentary sequence of the Murray Ridge provides an excellent archive of past primary productivity and Indian summer monsoon intensity (Pourmand et al., 2004; Reichart et al., 1997; Reichart et al., 1998; Reichart et al., 2004; Schulz et al., 1998). IMAGES Core MD04-2881 was recovered on 14 October 2004, from a water depth of 2387 m at the Murray Ridge (22°12′5″ N–63°5′5″ E) (Fig. 1). The sediment consists of homogeneous, dark brownish to olive greenish to light greenish/yellowish grey hemipelagic mud. The upper 34 m of the core have been sub-sampled in 10 cm resolution. XRF and magnetic susceptibility scans have been performed in 1 cm resolution.

2.2 Analytical methods

An Avaatech XRF core scanner at the Royal Netherlands Institute of Sea Research (NIOZ, Texel, Netherlands) has been used to measure the bulk elemental composition of the sediment core in high-resolution. The split core surface was cleaned and covered with a 4 µm thin SPEXCertiPrep Ultralene foil to avoid contamination and prevent desiccation. Each section was scanned four times at 0.1 mA/5 kV (no filter), 0.15 mA and 10 kV (no filter), 0.5 mA and 30 kV (Pd-thick filter) and 1 mA/50 kV (Cu-filter). A 1 cm^2 area of the core surface was irradiated with X-rays using 30 s count time (120 s for the 50 kV setup). For further technical details on the XRF scanning technique see (Richter et al., 2006).

Reliability of XRF scanning counts has been tested by comparing it to a lower-resolution sample set (10 cm) for XRF measurements on discrete samples. 3–5 g of freeze-dried sediment was thoroughly ground. Residual moisture, organic matter and carbonates were removed using a Leco TGA (Thermo-Gravimetric Analysis 600 mg of the residue was mixed with 6 g flux (consisting of 66% lithium tetraborate, $Li_2B_4O_7$ and 34% lithium metaborate, $LiBO_2$) and 0.500 ml of a 30% lithium iodide solution and fused to glass beads. Glass beads were measured using an ARL9400 X-ray fluorescence spectrometer. Analytical precision, as checked by parallel analysis of international reference material and in-house standards, is better than 2% for Al, Ti better than 3% for Ba.

In general, XRF scanning is less suited for light elements (Richter et al., 2006; Tjallingii et al., 2007). When comparing the elemental scanning counts for Al with the absolute measurements on discrete samples we find a low correlation (r^2=0.38). This low correlation coefficient implies that normalization to Aluminum (Al), which is commonly done for elemental data, will lead to large uncertainties for the XRF scanning dataset. We therefore rely only on the raw counts for barium (Ba), calcium (Ca), strontium (Sr), the sum of the terrestrial elements and bromine (Br).

Magnetic susceptibility of discrete samples was measured on a Kappabridge KLY-2. Susceptibility was divided by the sample's dry weight, giving the mass magnetic susceptibility [m^3/kg].

Stable isotope ratios were measured on the benthic foraminifera *Uvigerina peregrina* (single specimen, size fraction 150–600 µm) and the planktic foraminifera *Neogloboquadrina dutertrei* (~20 specimen, 300–350 µm) and *Globigerinoides ruber* (~50 specimen, 212–300 µm). Single specimen of the benthic foraminifera and aliquots of the homogenized *G. ruber* samples were loaded into individual reaction vessels, and each sample was reacted with three drops of H_3PO_4 (specific gravity=1.92) using a Finnigan MAT Kiel III carbonate preparation device, at Utrecht University. Long-term analytical precision was estimated to be ±0.07 for δ^{18}O and ±0.03 for δ^{13}C by measuring eleven standards (international NBS-19 and in house NAXOS) with each set of 38 samples. The *Neogloboquadrina* samples were analyzed in an ISOCARB common bath carbonate preparation device linked on-line to VG SIRA24 mass spectrometer also at Utrecht University. Isotope Values were calibrated to the PeeDeeBeleminte (PDB) scale. Analytical precision was determined by replicate analyses and by comparison to the international (IAEA-CO1) and in-house carbonate standard (NAXOS). Replicate analyses showed standard deviations of ±0.06 and ±0.1 for δ^{13}C and δ^{18}O, respectively.

Size-normalized weights of the planktic foraminiferal species *G. ruber* were measured to estimate the amount of carbonate dissolution. These measurements were done on the same relative narrow size fraction (212–300 µm) used for stable isotope analysis. The shells were weighed using a microbalance (precision 0.1 µg) and the mean weight is taken to represent that population.

Total numbers of the deep dwelling planktic foraminiferal species *Globorotalia truncatulinoides* and *Globoratalia crassaformis* were counted on splits of the 150–600 µm size fractions from the wet sieved freeze-dried sediment. Counts are expressed as number per gram dry sediment. Certain intervals of the core are characterized by high abundances of "green grains", which were counted on the same sample splits and are expressed as number per gram dry sediment.

3 Results

3.1 Chronology

Age constraints are based on correlating the benthic $\delta^{18}O$ *U. peregrina* record to the LR04 benthic oxygen isotope stack (Lisiecki and Raymo, 2005) (Fig. 2). This correlation shows that MD04-2881 covers the past ~750 000 years, although the oldest ~100 000 years are less well confined. The amplitude variations in the $\delta^{18}O$ *U. peregrina* record are comparable to the global benthic stack, except for the interval below ~600 ka, which shows only minor variations. The planktic $\delta^{18}O$ records from *N. dutertrei* and *G. ruber* largely confirm the benthic isotope chronology. We do not find exceptionally light isotope values in any of the two planktic records during MIS 14, thereby excluding an exceptional flooding event in the northern Indian Ocean during MIS 14 (Rossignol-Strick et al., 1998). We note also that, Bassinot et al. (1994) suggested that the isotope peaks in the equatorial Indian Ocean record are potentially related to an autochthonous sediment lens. Similar to the *U. peregrina* record, a dampened $\delta^{18}O$ signal is found in the record of N.dutertrei beyond ~650 ka. The resulting age model indicates that interglacial periods are characterized by lower sedimentation rates compared to glacial periods. Sedimentation rate is in particular low during MIS 5, which may even suffer from a hiatus.

The reason for the dampened isotopic signal in the lower part of the core has yet not been solved, but it is well known that the benthic isotope signal in the Arabian Sea has been altered by OMZ variability through changes in carbonate ion concentrations and supralysoclinal dissolution (Schmiedl and Mackensen, 2006). Furthermore, changes in Arabian Sea intermediate water masses between glacial and interglacial periods potentially influence the isotope signal (Jung et al., 2001; Zahn et al., 1991), although it is not clear why this would affect both benthic and planktic $\delta^{18}O$ records. Perhaps an increased diagenetic alteration of the isotopic signal with depth may have played a critical role. Clearly, the magnetic susceptibility record of MD04-2881 shows a decreasing down-core trend with flat values below ~650 ka (Fig. 2), indicating the diagenetic removal of the magnetic properties in the sediment by the decomposition of organic matter and associated changes in the redox conditions of the pore waters within this interval (Reichart et al., 1997).

3.2 OMZ intensity and productivity changes

Marine organic carbon (MOC) content of Murray Ridge sediment cores has previously been used as productivity and/or OMZ intensity proxy (Reichart et al., 1998). It has recently been shown that the Br counts from XRF scanning enabled a fast and robust procedure to estimate the MOC content of the sediment (Ziegler et al., 2008). The Br record of MD04-2881 indicates that maximum MOC contents occur during glacial periods, whereas the lowest values coincide with glacial terminations (Fig. 3). These minimum values are accompanied by peak occurrences of *G. crassaformis* and *G. truncatulinoides* (Fig. 3). *G. crassaformis* and *G. truncatulinoides* are deep-dwelling planktic foraminiferal species that reached high abundances in the Arabian Sea during extreme cold events in the North Atlantic (Reichart et al., 1998; Ziegler et al., 2009). Similar to the ice rafted debris layers in the North Atlantic, peak occurrences of the *Globorotalids* usually do not last for more than a few thousand years and their abundances always return to very low baseline values before rising again. It has been suggested that their occurrences are indicative for periods of intensified winter mixing due to extreme cold winter monsoons, resulting in a breakdown of the OMZ (Reichart et al., 1998). Others argued that evidence for the required salinity and/or sea surface temperature changes in such a mechanism are missing and that the winter mixing theory is therefore hypothetical (Schulte et al., 1999). These authors linked a break-down of the OMZ instead to processes in the global oceanic circulation. The interval from

470 to 570 ka is remarkable, as it is the longest interval in the record, where no *G. crassaformis* or *G. truncatulinoides* specimen occur.

Amongst others, Reichart et al. (1997, 1998) showed that the MOC content of the Murray Ridge records co-varies with other upwelling productivity indicators (e.g. *Globigerina bulloides* abundances and Ba/Al). Ba for instance has been successfully applied as proxy for primary productivity (Dehairs et al., 1980; Gingele et al., 1999; Jacot Des Combes et al., 1999; Shimmield and Mowbray, 1991). Barite crystals precipitate in microenvironments within decaying organic matter (Dehairs et al., 1980). One problem in the interpretation of Ba as productivity indicator lies in the distinction of biogenic and detrital Ba. Normalization with Al is therefore commonly used to assess the detrital Ba component e.g. (Gingele et al., 1999). The relative contribution of detrital Ba appears small at the Murray Ridge (Schenau et al., 2001), so that the Ba records we obtained from MD04-2881 by XRF scanning and discrete sampling will reflect primarily changes in productivity. Note that we will use primarily the raw counts for barium in our discussion, because they are highly correlated with the Ba/Al ratios derived from the discrete samples of the last 462 ka (Fig. 3).

Evidently, the Ba record co-varies with the benthic oxygen isotope record, indicating highest primary productivity conditions during interglacial periods as was previously found (Shimmield, 1992). This implies that the maximum MOC contents during glacial periods at the depth of our studied core are most likely related to other processes than increased productivity conditions only, as has been suggested for other Arabian Sea MOC records (Clemens and Prell, 2003; Murray and Prell, 1992; Schmiedl and Leuschner, 2005).

A comparison of sediment cores from different water depths at the Murray Ridge indicated that relatively shallow cores from within the modern OMZ contain the highest MOC contents during interglacial periods and that they vary in-phase with other productivity proxies, while the deeper sites (i.e., well below the present-day OMZ) contain the highest MOC contents during glacial periods (Ziegler et al., 2009). This suggests that the oxygen content of the bottom water at the core depth, and thereby the extension of the OMZ, is an important factor in controlling the depth dependent preservation of organic matter. Primary productivity is a second factor, which becomes dominant in records that are constantly within the OMZ. Higher sedimentation rates during glacial periods would have further facilitated the preservation of organic carbon (Clemens and Prell, 2003), but this process cannot explain the differences in MOC content between various water depths. On this basis, we may conclude that the Br enrichments during glacial periods in MD04-2881 coincide with an extreme downward extension of the OMZ. In turn, the relative low Ba concentrations within the MOC maxima during glacial periods could be due to early diagenesis processes. Arabian Sea sediments that are deposited well within the modern OMZ are characterized by high C_{org}/Ba_{bio} ratios, because of a lower preservation of Barite upon deposition through sulfate-reducing conditions (Schenau et al., 2001).

3.3 Dissolution and dilution processes

Bulk elemental concentrations of Ca and Sr versus the sum of Al, Si, Ti, Fe and K reflect the input and preservation of biogenic carbonate versus the relative input of terrestrial material (Fig. 3). Because of its elevated location, the site is shielded from the input of turbidities and fan sedimentation of the Indus. The terrestrial material is therefore most likely wind derived (Reichart et al., 1997). Changes in the Ti/Al ratio of the sediments from the Murray Ridge have been applied in former studies as indicator for grain size and thus wind speed, since Titanium is concentrated in heavy minerals in the coarser size fraction (Reichart et al., 1997). The Ti/Al record of MD04-2881 shows a close relationship with the glacial-interglacial variability (Fig. 3) as was previously been found for the Oman Margin, with higher Ti/Al values corresponding to an increased coarse-grained lithogenic flux into the Arabian Sea during dry glacial periods (Clemens et al., 1996). The total concentration of terrestrial elements in MD04-2881 shows however no clear glacial-interglacial variability. Several interglacial periods are even characterized by increased terrestrial element concentrations. This suggests that the bulk variations in terrestrial elements are dominated by the production and preservation of biogenic

CPD
5, 1989–2018, 2009

carbonate rather than by dilution.

Increased Ca and Sr contents and lower contents of terrestrial elements characterize the MBDI from 280 to 480 ka, with the exception of MIS 11 (Fig. 3). Similar to MD04-2881, this carbonate plateau has been found in other Indian Ocean cores and was related to long-term eccentricity-driven cycles in the production of coccolithopores (Rickaby et al., 2007). Extreme minimum Ca and Sr contents coincide with MIS 5 and 13. These interglacial periods are characterized by the lowest sedimentation rates and hence point to periods of severe carbonate dissolution (Fig. 3).

Calcite dissolution may occur above the lysocline when the metabolic release of CO_2 during organic matter remineralization leads to carbonate under-saturation in the pore waters (Adler et al., 2001; Jahnke et al., 1994). This supralysocline dissolution process typically occurs below the OMZ in the Arabian Sea, where a high flux of organic material is accompanied by oxygen availability (Klöcker et al., 2007; Schulte and Bard, 2003; Tachikawa et al., 2008). The water depth of the studied core at around 2400 m was apparently strongly influenced by supralysoclinal dissolution during interglacial periods, when productivity conditions were significantly enhanced.

Size normalized weights (SNW) of planktic foraminifera have been used as indicator for surface (Barker and Elderfield, 2002) and bottom water carbonate ion concentration $[CO_3^{2-}]$ (Broecker and Clark, 2001; Lohmann, 1995). The SNW of *G. ruber* shows a good correlation with the Ba record, but also with the extensive OMZ intensities during the glacial periods (Fig. 3). This suggests that the SNW records may represent an even better picture of productivity variations in the Arabian Sea than the Ba record, which could have been altered during extended OMZ conditions (see above). Anomalous low SNW values are found during MIS 13. Due to the complete dissolution of foraminifers during MIS 5, no SNW data could be obtained from this interval.

MIS 5 and 13 are furthermore characterized by large numbers of light green to dark green grains in the sand size fraction (Fig. 3). Green grains commonly occur at the edges of oxygen-minimum zones and are composed of authigenic minerals, most commonly Glauconite (Kelly and Webb, 1999; Mullins et al., 1985). They often form within granular substrates such as faecal pellets or foraminiferal chambers. Glauconite forms at or near the sediment surface and requires low sedimentation rates, so that enough time is available for biological alteration of detrital clay minerals (Worden and Morad, 2003). The process of glauconization is often associated with relatively shallow water depths (<1000 m). The core depth of 2347 m is to our knowledge one of the deepest water depth where in-situ glauconite formation has been found yet (see also Wiewiora et al., 2001).

4 Discussion

4.1 Intensity of the Indian-Asian monsoon

The atmospheric methane record from Antarctic ice cores reflects largely the strength of tropical monsoon with a secondary input from boreal sources (Loulergue et al., 2008; Ruddiman and Raymo, 2003). Widespread wetlands during periods of increased summer monsoon precipitation are an important source of methane production when organic material decays under reducing conditions. We consider therefore the methane record as the backbone or target curve for the interpretation of the productivity changes and associated supralysocline dissolution intervals in our studied core from the Arabian Sea.

The longest methane record currently achieved comes from EPICA Dome C, which covers the last 800 000 years (Fig. 4). Changes in methane concentrations are dominated by the ~100 ka glacial rhythm superimposed on the 23 ka precession component (Loulergue et al., 2008; Spahni et al., 2005). The strong imprint of the precession cycle is consistent with the outcome of climate model experiments, which indicate that tropical monsoons respond primarily to changes in Northern Hemisphere summer insolation on orbital timescales (Kutzbach, 1981). Recently, we carried out a transient simulation with the intermediate complexity model CLIMBER-2 that included both insolation and ice volume variations (Tuenter et al., unpublished data; Ziegler et al., 2009).

Indeed, this simulation reveals that the intensity of Indian-Asian summer monsoon precipitation responds to both forcing parameters, in accord with the Antarctic methane record over the past 650 ka (Fig. 4).

Overall, the variations in Ba and SNW records of MD04-2881 share many features with the methane record and model simulation, from which one could conclude that the productivity changes in the Arabian Sea primarily reflect changes in summer monsoon upwelling and associated changes in the carbonate ion concentration of the water (Fig. 4). A marked exception, however, is the anomalous high productivity peak and carbonate dissolution event associated with MIS 13. During this time, methane concentrations are lower than in every other interglacial period of the last 500 000 years (Fig. 4). Also from a modelling perspective, the extreme summer monsoon maximum in MIS 13 is unexpected, because (1) benthic isotope records indicate that MIS 13 is a relatively cool interglacial (Lisiecki and Raymo, 2005), with remnant ice sheets in the Northern Hemisphere, and (2) Northern Hemisphere summer insolation maxima are not particularly strong in this period, although the earth's eccentricity was at a maximum around 500 ka (Laskar et al., 1993).

4.2 Inferences from the Chinese loess plateau

The Chinese loess plateau (CLP) is an important climate archive for the reconstruction of the Asian summer and winter monsoon as far back as 22 million years ago (Ding et al., 1995; Guo et al., 2002; Kukla et al., 1988; Porter and An, 1995). The winter monsoon transports dust from the Asian inlands to the CLP, while the summer monsoon brings precipitation (Porter and An, 1995). Successive loess and soil layers are therefore interpreted as alternating periods of strengthened winter (cold and dry) and summer monsoon (wet and warm), respectively. Recently it has been suggested that it is actually the breakdown of the Siberian High during spring that produces windstorms and associated dust deposition (Roe, 2009). Most proxies that have been used to unravel the history of the loess sequence (e.g. magnetic susceptibility) reflect the degree of chemical weathering and thus soil formation (Liu and Ding, 1998). Many loess records are dominated by glacial-interglacial variability superimposed by millennial scale events, which correlate to Heinrich events (Ding et al., 1995; Liu and Ding, 1998; Porter and An, 1995).

The Ba and, to a lesser degree, SNW records of MD04-2881 show a high similarity with a magnetic susceptibility stack from the CLP (Clemens et al., 2008). This confirms our interpretation that they reflect primarily summer monsoon upwelling-related productivity variations that are paced by glacial-interglacial variability and Northern Hemisphere summer insolation changes (Fig. 4). In contrast to the Antarctic methane record and model simulation, the exceptional high productivity conditions reached during MIS 13 coincide with an exceptional thick soil horizon S5 in some loess records of the central CLP (Guo et al., 2000; Sun et al., 2006b), and with an extreme event in a monsoon record from the Tibetan plateau (Chen et al., 1999). There are however noticeable regional differences in the expression of the S5 soil horizon (Sun et al., 2006a). While records from the central CLP expose a thick well developed soil horizon, the S5 is hardly detected in the northwestern area. It was suggested that maximum intensities of summer monsoon precipitation did not reach this region until MIS 11 (Sun et al., 2006a). The latter observation is in much better agreement with the Antarctic methane record, which shows that methane concentrations were significantly lower during MIS 13 than during the interglacial periods after the Mid-Brunhes event, MBE, at ~430 ka (Loulergue et al., 2008; Spahni et al., 2005).

Another major difference between the loess records of the central and northwestern site of the CLP is that in the central region soil occurrences are determined by glacial-interglacial variability, while they exhibit a strong precession imprint in the northwest (Sun et al., 2006a). The latter observation is not only in good agreement with the Antarctic methane record, but also with the Indian-Asian summer monsoon reconstructions derived from the Chinese speleothem oxygen isotope records of the Sanbao and Hulu caves, which indicate primarily 23 ka precession cycles over the last 225 000 years (Wang et al., 2008). Similar to the loess records, the speleothem-derived monsoon record is overprinted by rapid events, which occur synchronously with climate variations in the North Atlantic region (Wang et al., 2005b; Wang et al., 2001).

4.3 Cause of the extensive productivity conditions during MIS 13

Comparison of the Chinese loess records with temperature records from Antarctica have led to the suggestion that the climates of both hemispheres are unusual asymmetric during MIS 13 (Guo et al., 2009). Accordingly, Northern Hemisphere mean annual temperatures, evidenced by extremely soil formation in the Loess Plateau record, weakest Asian winter monsoon, and lowest Asian dust and iron fluxes, were much warmer than at the Southern Hemisphere, because the global oxygen isotope record is characterized by relatively positive values (Guo et al., 2009). Moreover the Deuterium (δD) record of the EPICA Dome C ice core showed relatively cold interglacial temperatures during MIS 13, indicating that at least Antarctic temperatures were cold with respect to the successive interglacial periods (Jouzel et al., 2007). On the other hand, data from a glaciomarine sedimentary sequence from the West Antarctic continental margin suggest that the interval spanning MIS 15–13 was one single, prolonged interglacial period, which potentially experienced a collapse of the West Antarctic Ice sheet (Hillenbrand et al., 2009).

Warm Northern Hemisphere annual temperatures are consistent with the continuous forestation and inferred reduced mountain glaciations in central Eurasia throughout MIS 15 to 11 (Prokopenko et al., 2002). Tree growth is particularly sensitive to wintertime climate. Therefore this period was probably characterized by mild winters, with relatively little snow cover. Such mild winter conditions would explain the absence of *G. crassaformis* or *G. truncatulinoides* in our Arabian Sea record in this interval. In addition, the higher winter temperatures may explain the thick soil horizon S5 in the central CLP. First it may facilitate pedogenesis through enhanced chemical weathering, and secondly a less intense winter monsoon may lead to a reduction of dust flux to the loess sites. As an alternative explanation from a modelling study, it was suggested that a precipitation maximum during MIS 13 could have occurred because of a reinforcement of the summer monsoon by an intermediate sized Eurasian ice-sheet (Yin et al., 2008). Such a scenario, however does not explain the regional differences between the loess records and absence of a distinct monsoon event in the EPICA methane record during MIS 13. We therefore suggest that the anomalous climate patterns observed worldwide during MIS 13 are not primarily linked to changes in the intensity of the monsoon, but reflect an important turnover in the Atlantic circulation.

During the interim state of the MPT, the formation of North Atlantic deep water (NADW) was decreased and deep waters were influenced by a large Southern Hemisphere component (Raymo et al., 1997; Schmieder et al., 2000). Around T_{VI}, a series of events occurred in the South Atlantic, which point to a significant increase in NADW formation during that time (Gingele and Schmieder, 2001; Romero and Schmieder, 2006; Schmieder et al., 2000): (1) A very high production of NADW has been inferred from globally distributed benthic carbon isotope records (Raymo et al., 1997). (2) During MIS 13 an extreme $\delta^{13}C_{max}$ occurs, which has been interpreted as a major reorganization in the carbon reservoir of the global ocean (Wang et al., 2001). (3) A certain group of benthic foraminifera became extinct (Gupta et al., 2006; Kawagata et al., 2006). (4) An increased poleward heat transport in the Atlantic Ocean has been evidenced by pollen records offshore Greenland (de Vernal and Hillaire-Marcel, 2008). These records suggest that the size of the Greenland ice-sheet was much more reduced than today, even though the benthic isotope record indicates a larger global ice volume during MIS 13.

A modelling study showed that an increased NADW formation affects the primary productivity and OMZ intensity in the Arabian Sea through increased nutrient availability on millennial time scales (Schmittner et al., 2007). In a separate study, it has been already suggested that primary productivity changes in the Arabian Sea on orbital timescales are more sensitive to the global ocean circulation than to the summer monsoon intensity, and therefore displays a much longer precession phase-lag (Ziegler et al., 2009). In analogy, we propose that the productivity peak and associated anomalous dissolution event during MIS 13 relates to the increased Atlantic overturning circulation around T_{VI}. At the same time the increased heat transport to high northern latitudes might have caused the exceptionally mild winter conditions in Eurasia. Denton et al. (2005) suggested that the winter climate was much more sensitive to past changes in the Atlantic meridional overturning, due to sea-ice feedback mechanisms. Mild winter temperatures facilitated probably the soil formation in the central CLP. This implies that not only Arabian Sea productivity but also the soil formation in the CLP was decoupled from the Asian summer monsoon intensity during MIS 13.

5 Conclusions

A high-resolution multi-proxy record from the northeastern Arabian Sea of the past 750 ka reveals productivity changes, which oscillate primarily in concert with the ~100 ka glacial-interglacial rhythm. Highest productivity peaks are associated with interglacial periods. In contrast, the base of the OMZ deepens during glacial periods, suggesting that intermediate water ventilation played an important role. Termination T_{VI} differs from the other major late Pleistocene terminations (T_{I-V} and T_{VII}) by the absence of a strong winter monsoon-related event in the Arabian Sea. An intensive Atlantic overturning circulation during this time may have been responsible for the mild winter conditions found in large parts of the Northern Hemisphere, and thereby the weakened Asian winter monsoon. In turn, enhanced NADW production during T_{VI} may have increased the supply of nutrients to the Arabian Sea, thereby setting the stage for the anomalously high productivity conditions and carbonate dissolution event during MIS 13.

Acknowledgements. This study is supported by the Research Council for Earth and Life Sciences (ALW) with financial aid from the Netherlands Organization for Scientific Research (NWO) to L. J. Lourens (grants 853.00.032 and 834.04.003). A. van Dijk, R. Giles, G. Ittmann, T. Richter and A. Vaars are thanked technical support. We thank Frits Hilgen for comments on an earlier version of the manuscript. J.-W. Zachariasse, initiator of the CHAMAK-IODP cruise is in particularly acknowledged as well as the other crewmembers of R/V M. Dufresne and NIOZ technicians for their shipboard support.

References

Adler, M., Hensen, C., Wenzhoefer, F., Pfeifer, K., and Schulz, H. D.: Modeling of calcite dissolution by oxic respiration in supralysoclinal deep-sea sediments, Mar. Geol., 177(1–2), 167–189, 2001.

Almogi-Labin, A., Schmiedl, G., Hemleben, C., Siman-Tov, R., Segl, M., and Meischner, D.: The influence of the NE winter monsoon on productivity changes in the Gulf of Aden, NW Arabian Sea, during the last 530 ka as recorded by *foraminifera*, Mar. Micropaleontol., 40(3), 295–319, 2000.

Altabet, M. A., Higginson, M. J., and Murray, D. W.: The effect of millennial-scale changes in Arabian Sea denitrification on atmospheric CO_2, Nature, 415(6868), 159–162, 2002.

Anderson, D. M., Overpeck, J. T., and Gupta, A. K.: Increase in the Asian Southwest monsoon during the past four centuries, Science, 297(5581), 596–599, 2002.

Barker, S., Archer, D., Booth, L., Elderfield, H., Henderiks, J., and Rickaby, R. E. M.: Globally increased pelagic carbonate production during the Mid-Brunhes dissolution interval and the CO_2 paradox of MIS 11, Quaternary Sci. Rev., 25, 3278–3293, 2006.

Barker, S. and Elderfield, H.: Foraminiferal calcification response to glacial-interglacial changes in atmospheric CO_2, Science, 297(5582), 833–836, 2002.

Bassinot, F. C., Labeyrie, L. D., Vincent, E., Quidelleur, X., Shackleton, N. J., and Lancelot, Y.: The astronomical theory of climate and the age of the Brunhes-Matuyama magnetic reversal, Earth Planet. Sc. Lett., 126(1–3), 91–108, 1994.

Bollmann, J., Baumann, K. H., and Thierstein, H. R.: Global dominance of *Gephyrocapsa coccoliths* in the late Pleistocene: selective dissolution, evolution or global environmental change? Paleoceanography, 13, 517–529, 1998.

Broecker, W. and Clark, E.: An evaluation of Lohmann's *foraminifera* weight dissolution index, Paleoceanography, 16(5), 531–534, 2001.

Budziak, D., Schneider, R. R., Rostek, F., Muller, P. J., Bard, E., and Wefer, G.: Late quaternary insolation forcing on total organic carbon and C-37 alkenone variations in the Arabian Sea, Paleoceanography, 15(3), 307–321, 2000.

Chen, F. H., Bloemendal, J., Zhang, P. Z., and Liu, G. X.: An 800 ky proxy record of climate from lake sediments of the Zoige Basin, eastern Tibetan Plateau, Palaeogeogr. Palaeocl., 151, 307–320, 1999.

Clark, P. U., Archer, D., Pollard, D., Blum, J. D., Rial, J. A., Brovkin, V., Mix, A., Pisias, N. G., and

Roy, M.: The middle Pleistocene transition: characteristics, mechanisms, and implications for long-term changes in atmopheric pCO_2, Quaternary Sci. Rev., 25, 3150–3184, 2006.
Clemens, S., Prell, W., Murray, D., Shimmield, G., and Weedon, G.: Forcing mechanisms of the Indian Ocean monsoon, Nature, 353(6346), 720–725, 1991.
Clemens, S. C., Murray, D. W., and Prell, W. L.: Nonstationary phase of the Plio-Pleistocene Asian monsoon. Science, 274(5289), 943–948, 1996.
Clemens, S. C. and Prell, W. L.: Late Pleistocene variability of Arabian Sea summer monsoon winds and continental aridity: Eolian records from the lithogenic component of deep-sea sediments, Paleoceanography, 5(2), 109–145, 1990.
Clemens, S. C. and Prell, W. L.: A 350 000 year summer-monsoon multi-proxy stack from the Owen Ridge, Northern Arabian Sea, Mar. Geol., 201(1–3), 35–51, 2003.
de Vernal, A. and Hillaire-Marcel, C.: Natural variability of Greenland climate, vegetation, and ice volume during the past million years, Science, 320(5883), 1622–1625, 2008.
Dehairs, F., Chesselet, R., and Jedwab, J.: Discrete suspended particles of barite and the barium cycle in the open ocean, Earth Planet. Sc. Lett., 49, 528–550, 1980.
Denton, G. H., Alley, R. B., Comer, G. C., and Broecker, W. S.: The role of seasonality in abrupt climate change, Quaternary Sci. Rev., 24(10–11), 1159–1182, 2005.
Ding, Z. L., Liu, T. S., Rutter, N. W., Yu, Z. W., Guo, Z. T. and Zhu, R. X.: Ice-volume forcing of East Asian winter monsoon variations in the past 800 000 years, Quaternary Res., 44, 149–159, 1995.
Droxler, A. W., Ferro, E. C., Mucciarone, D. A., and Haddad, G. A.: The marine carbonate system during oxygen isotope stage 11 (423–362 ka): a case of basin-to-shelf and/or basin-to-basin carbonate fractionation? EOS, Trans. Am. Geophys. Union, 78, 179, 1997.
Droxler, A. W., Haddad, G. A., Mucciarone, D. A., and Cullen, J. L.: Pliocene-Pleistocene variations in aragonite content and planktonic oxygen-isotope record in Bahamian periplatform ooze, Hole 633A. Proceedings of the Ocean Drilling Program, Scientific Results, 101, 221–244, 1988.
Emeis, K., Anderson, D. M., Doose, H., Kroon, D., and Schulz-Bull, D.: Sea-surface tempertures and the history of monsoon upwelling in the Northwest Arabian Sea during the last 500 000 years, Quaternary. International, 43, 355–361, 1995.
Gingele, F. X. and Schmieder, F.: Anomalous South Atlantic lithologies confirm global scale of unusual mid-Pleistocene climate excursion, Earth Planet. Sc. Lett., 186, 93–101, 2001.
Guo, Z. T., Berger, A., Yin, Q. Z., and Qin, L.: Strong asymmetry of hemispheric climates during

MIS-13 inferred from correlating China loess and Antarctica ice records, Clim. Past, 5, 21–31, 2009, http://www.clim-past.net/5/21/2009/.
Guo, Z. T., Biscaye, P., Wei, L. Y., Chen, X. H., and Peng, S. Z.: Summer monsoon variations over the last 1.2 Ma from the weathering of loess-soil sequences in China, Geopys. Res. Lett., 27, 1751–1754, 2000.
Guo, Z. T., Ruddiman, W. F., Hao, Q. Z., Wu, H. B., Qiao, Y. S., Zhu, R. X., Peng, S. Z., Wei, J. J., Yuan, B. Y., and Liu, T. S.: Onset of Asian desertification by 22 Myr ago inferred from loess deposits in China, Nature, 416, 159–163, 2002.
Gupta, A. K., Anderson, D. M., and Overpeck, J. T.: Abrupt changes in the Asian Southwest monsoon during the Holocene and their links to the North Atlantic Ocean, Nature, 421(6921), 354–357, 2003.
Gupta, A. K., Sarkar, S., and Mukherjee, B.: Paleoceanographic changes during the past 1.9 Myr at DSDP site 238, Central Indian Ocean Basin: Benthic foraminiferal proxies, Mar. Micropaleontol., 60(2), 157–166, 2006.
Harris, S. E., Mix, A., and King, T.: Biogenic and terrigenous sedimentation at Ceara Rise, western tropical Atlantic, supports Pliocene-Pleistocene deep-water linkage between hemispheres, Proceedings of the Ocean Drilling Program. Scientific Results, 154, 331–345, 1997.
Hillenbrand, C.-D., Kuhn, G., and Friederichs, T.: Record of a mid-Pleistocene depositional anomaly in West Antarctic continental margin sediments: In indicator for ice-sheet collapse? Quaternary Sci. Rev., 28, 1147–1159, 2009.
Hönisch, B., Hemming, N. G., Archer, D., Siddall, M., and McManus, J.: Atmospheric carbon dioxide concentration across the mid-Pleistocene transition, Science, 324, 1551–1554, 2009.
Ishikawa, S. and Motoyoshi, O.: Reconstruction of Indian monsoon variability over the past 230 000 years: Planktic foraminiferal evidence from the NW Arabian Sea open-ocean upwelling area, Mar. Micropaleontol., 63, 143–154, 2007.
Ivanova, E. M., Schiebel, R., Deo Singh, A., Schmiedl, G., Niebler, H.-S., and Hemleben, C.: Primary production in the Arabian Sea during the last 135 000 years, Palaeogeogr. Palaeocl., 197, 61–82, 2003.
Jacot Des Combes, H., Caulet, J. P., and Tribovillard, N. P.: Pelagic productivity changes in the equatorial area of the northwest Indian Ocean during the last 400 000 years, Mar. Geol.,

158, 27–55, 1999.
Jaeschke, A., Ziegler, M., Hopmans, E. C., Reichart, G. J., Lourens, L. J., Schouten, S., and Sinninghe Damste, J. S.: Molecular fossil evidence for anaerobic ammonium oxidation in the Arabian Sea over the last glacial cycle, Paleoceanography, 24, PA2202, doi:10.1029/2008PA001712, 2009.
Jahnke, R., Craven, D. B., and Gaillard, J.-F.: The influence of organic matter diagenesis on $CaCO_3$ dissolution at the dee-sea floor, Geochim. Cosmochim. Ac., 58(13), 2799–2809, 1994.
Jouzel, J., Masson-Delmotte, V., Cattani, O., Dreyfus, G., Falourd, S., Hoffmann, G., Minster, B., Nouet, J., Barnola, J. M., Chappellaz, J., Fischer, H., Gallet, J. C., Johnsen, S., Leuenberger, M., Loulergue, L., Luethi, D., Oerter, H., Parrenin, F., Raisbeck, G., Raynaud, D., Schilt, A., Schwander, J., Selmo, E., Souchez, R., Spahni, R., Stauffer, B., Steffensen, J. P., Stenni, B., Stocker, T. F., Tison, J. L., Werner, M., and Wolff, E. W.: Orbital and millennial Antarctic climate variability over the past 800 000 Years, Science, 317(5839), 793–796, 2007.
Jung, S. J. A., Ganssen, G. M., and Davies, G. R.: Multidecadal variations in the early Holocene outflow of Red Sea Water into the Arabian Sea, Paleoceanography, 16(6), 658–668, 2001.
Kawagata, S., Hayward, B. W., and Gupta, A. K.: Benthic foraminiferal extinctions linked to late Pliocene-Pleistocene deep-sea circulation changes in the northern Indian Ocean (ODP sites 722 and 758), Mar. Micropaleontol., 58(3), 219–242, 2006.
Kelly, J. C. and Webb, J. A.: The genesis of glaucony in the Oligo-Miocene Torquay group, southeastern Australia: Petrographic and geochemical evidence, Sediment. Geol., 125(1–2), 99–114, 1999.
Klöcker, R., Ivanochko, T. S., Brummer, G.-J., Jung, S. J. A., Ganssen, G., Kroon, D., Ganeshram, R. S., and Henrich, R.: Variation in production, input and preservation of metastable calcium carbonate off Somalia during the last 90 000 years, Quaternary Sci. Rev., 26(19–21), 2674–2683, 2007.
Kukla, G., Heller, F., Ming, L. X., Chun, X. T., Sheng, L. T., and Sheng, A. Z.: Pleistocene climates in China dated by magnetic susceptibility, Geology, 16, 811–814, 1988.
Kutzbach, J. E.: Monsoon climate of the early Holocene: climate experiment with Earth's orbital parameters for 9000 years ago, Science, 214, 59–61, 1981.
Laskar, J., Joutel, F., and Boudin, F.: Orbital, precessional, and insolation quantities for the Earth from −20 Myr to +10 Myr, Astron. Astrophys., 270(1–2), 522–533, 1993.
Leuschner, D. C. and Sirocko, F.: The low-latitude monsoon climate during Dansgaard–

CPD
5, 1989–2018, 2009

Anomalously high Arabian Sea productivity conditions

M. Ziegler et al.

Oeschger cycles and Heinrich events, Quaternary Sci. Rev., 19, 243–254, 2000.
Leuschner, D. C. and Sirocko, F.: Orbital insolation forcing of the Indian Monsoon – a motor for global climate changes? Palaeogeogr. Palaeocl., 197, 83–95, 2003.
Liu, T. and Ding, Z.: Chinese loess and the paleomonsoon, Annu. Rev. Earth Planet. Sci., 26, 111–145, 1998.
Lohmann, G. P.: A Model for variation in the chemistry of planktonic *foraminifera* Due to secondary calcification and selective dissolution, Paleoceanography, 10(3), 445–457, 1995.
Loulergue, L., Schilt, A., Spahni, R., Masson-Delmotte, V., Blunier, T., Lemieux, B., Barnola, J.-M., Raynaud, D., Stocker, T. F., and Chappellaz, J.: Orbital and millennial-scale features of atmospheric CH_4 over the past 800 000 years. Nature, 453(7193), 383–386, 2008.
Lückge, A., Doose-Rolinski, H., Khan, A. A., Schulz, H., and von Rad, U.: Monsoonal variability in the northeastern Arabian Sea during the past 5000 years: Geochemical evidence from laminated sediments, Palaeogeogr. Palaeocl., 167(3–4), 273–286, 2001.
Mullins, H. T., Thompson, J. B., McDougall, K., and Vercoutere, T. L.: Oxygen-minimum zone edge effects: Evidence from the central California coastal upwelling system, Geology, 13, 491–494, 1985.
Naidu, P. D.: Link between western Arabian Sea surface temperature and summer monsoon strength and high-latitude abrupt climate events, J. Geol. Soc. India, 68(3), 379–385, 2006.
Naidu, P. D. and Malmgren, B. A.: A high-resolution record of late Quaternary upwelling along the Oman Margin, Arabian Sea based on planktonic *foraminifera*, Paleoceanography, 11(1), 129–140, 1996.
Pattan, J. N., Masuzawa, T., Naidu, P. D., Parthiban, G. and Yamamoto, M.: Productivity fluctuations in the southeastern Arabian Sea during the last 140 ka, Palaeogeogr. Palaeocl., 193, 575–590, 2003.
Petit, J. R.: Climate and atmospheric history of the past 420 000 years from the Vostok ice core, Antarctica, Nature, 399, 429–436, 1999.
Porter, S. C. and An, Z.: Correlation between climate events in the North Atlantic and China during the last glaciation, Nature, 375(6529), 305–308, 1995.
Pourmand, A., Marcantonio, F., and Schulz, H.: Variations in productivity and eolian fluxes in the northeastern Arabian Sea during the past 110 ka, Earth Planet. Sc. Lett., 221, 39–54, 2004.
Prabhu, C. N. and Shankar, R.: Palaeopruductivity of the eastern Arabian Sea during the past 200 ka: A multi-proxy investigation, Deep-Sea Res. Pt. II, 52, 1994–2002, 2005.

Prell, W. L. and Campo, E. V.: Coherent response of Arabian Sea upwelling and pollen transport to late Quaternary monsoonal winds. Nature, 323(6088), 526–528, 1986.
Prell, W. L., Hutson, W. H., Williams, D. F., Be, A. W. H., Geitzenauer, K., and Molfino, B.: Surface circulation of the Indian Ocean during the last glacial maximum, approximately 18 000 yr BP, Quaternary Res., 14(3), 309–336, 1980.
Prell, W. L. and Kutzbach, J. E.: Sensitivity of the Indian monsoon to forcing parameters and implications for its evolution, Nature, 360(6405), 647–652, 1992.
Prokopenko, A. A., Williams, D. F., Kuzmin, M. I., Karabanov, E. B., Khursevich, G. K., and Peck, J. A.: Muted climate variations in continental Siberia during the mid-Pleistocene epoch, Nature, 418(6893), 65–68, 2002.
Raymo, M. E., Lisiecki, L. E., and Nisancioglu, K. H.: Plio-Pleistocene ice volume, Antarctic climate, and the global {delta}18O record, Science, 313, 492–495, 2006.
Raymo, M. E., Oppo, D. W., and Curry, W.: The mid-Pleistocene climate transition: A deep sea carbon isotopic perspective, Paleoceanography, 12(4), 546–559, 1997.
Reichart, G. J., Brinkhuis, H., Huiskamp, F., and Zachariasse, W. J.: Hyperstratification following glacial overturning events in the northern Arabian Sea, Paleoceanography, 19(2), PA2013, doi:10.1029/2003PA000900, 2004.
Reichart, G. J., den Dulk, M., Visser, H. J., Van der Weijden, C. H., and Zachariasse, W. J.: A 225 kyr record of dust supply, paleoproductivity and the oxygen minimum zone from the Murray ridge (northern Arabian sea), Palaeogeogr. Palaeocl., 134(1–4), 149–169, 1997.
Reichart, G. J., Lourens, L. J., and Zachariasse, W. J.: Temporal variability in the northern Arabian Sea Oxygen Minimum Zone (OMZ) during the last 225 000 years, Paleoceanography, 13(6), 607–621, 1998.
Reichart, G. J., Schenau, S. J., De Lange, G. J., and Zachariasse, W. J.: Synchroneity of oxygen minimum zone intensity on the Oman and Pakistan margins at sub-Milankovitch time scales (vol. 185, pg. 283, 2002), Mar. Geol., 192(4), 437–438, 2002.
Rickaby, R. E. M., Bard, E., Sonzogni, C., Rostek, F., Beaufort, L., Barker, S., Rees, G., and Schrag, D. P.: Coccolith chemistry reveals secular variations in the global ocean carbon cycle? Earth Planet. Sc. Lett., 253, 83–95, 2007.
Roe, G.: On the interpretation of Chinese loess as a paleoclimate indicator, Quaternary Res., 71, 150–161, 2009.
Romero, O. and Schmieder, F.: Occurence of thick Ethmodiscus oozes associated with a terminal mid-Pleistocene transition event in the oligotrophic subtropical South Atlantic, Palaeo-

geogr. Palaeocl., 235, 321–329, 2006.
Rossignol-Strick, M., Paterne, M., Bassinot, F. C., Emeis, K., and De Lange, G. J.: An unusual mid-Pleistocene monsoon period over Africa and Asia, Nature, 392, 269–272, 1998.
Rostek, F., Bard, E., Beaufort, L., Sonzogni, C., and Ganssen, G.: Surface temperature and productivity records for the past 240 kyr in the Arabian Sea, Deep Sea Res. II, 44, 1461–1480, 1997.
Rostek, F., Ruhlandt, G., Bassinot, F. C., Muller, P. J., Labeyrie, L. D., Lancelot, Y., and Bard, E.: Reconstructing sea surface temperature and salinity using δ^18O and alkenone records, Nature, 364(6435), 319–321, 1993.
Ruddiman, W. F. and Raymo, M.: A methane-based time scale for Vostok ice, Quaternary Sci. Rev., 22, 141–155, 2003.
Saher, M. H., Jung, S. J. A., Elderfield, H., Greaves, M. J., and Kroon, D.: Sea surface temperatures of the western Arabian Sea during the last deglaciation, Paleoceanography, 22, PA2208, doi:10.1029/2006PA001292, 2007.
Sarkar, A., Ramesh, R., Bhattacharya, S. K., and Rajagopalan, G.: Oxygen isotope evidence for a stronger winter monsoon current during the last glaciation, Nature, 343(6258), 549–551, 1990.
Schenau, S. J., Prins, M. A., De Lange, G. J., and Monnin, C.: Barium accumulation in the Arabian Sea: Controls on barite preservation in marine sediments, Geochim. Cosmochim. Ac., 65(10), 1545–1556, 2001.
Schmieder, F., von Dobeneck, T., and Bleil, U.: The mid-Pleistocene climate transition as documented in the deep South Atlantic Ocean: Initiation, interim state and terminal event. Earth Planet. Sc. Lett., 179(3–4), 539–549, 2000.
Schmiedl, G. and Leuschner, D. C.: Oxygenation changes in the deep western Arabian Sea during the last 190 000 years: Productivity versus deepwater circulation, Paleoceanography, 20(2), 1–14, 2005.
Schmittner, A., Galbraith, E. D., Hostetler, S. W., Pedersen, T. F., and Zhang, R.: Large fluctuations of dissolved oxygen in the Indian and Pacific oceans during Dansgaard–Oeschger oscillations caused by variations of North Atlantic deep water subduction, Paleoceanography, 22, PA3207, doi:10.1029/2006PA001384, 2007.
Schulte, S. and Bard, E.: Past changes in biologically mediated dissolution of calcite above the chemical lysocline recorded in Indian Ocean sediments, Quaternary Sci. Rev., 22, 1757–1770, 2003.

Schulte, S., Rostek, F., Bard, E., Rullkotter, J., and Marchal, O.: Variations of oxygen-minimum and primary productivity recorded in sediments of the Arabian Sea, Earth Planet. Sc. Lett., 173(3), 205–221, 1999.
Schulz, H., von Rad, U., and Erlenkeuser, H.: Correlation between Arabian Sea and Greenland climate oscillations of the past 110 000 years, Nature, 393(6680), 54–57, 1998.
Shackleton, N. and Opdyke, N. D.: Oxygen-isotope and paleomagnetic stratigraphy of Pacific core V28-239: Late Pliocene to latest Pleistocene, Geol. Soc. Am. Mem., 145, 449–464, 1976.
Sirocko, F., Garbe-Schönberg, D., McIntyre, A., and Molfino, B.: Teleconnections between the subtropical monsoons and high-latitude climates during the last deglaciation, Science, 272, 526–529, 1996.
Sirocko, F., Sarnthein, M., Erlenkeuser, H., Lange, H., Arnold, M., and Duplessy, J. C.: Century-scale events in monsoonal climate over the past 24 000 years, Nature, 364, 322–324, 1993.
Spahni, R., Chappellaz, J., Stocker, T. F., Loulergue, L., Hausammann, G., Kawamura, K., Fluckiger, J., Schwander, J., Raynaud, D., Masson-Delmotte, V., and Jouzel, J.: Atmospheric methane and nitrous oxide of the late Pleistocene from Antarctic ice cores, Science, 310, 1317–1321, 2005.
Sun, Y., Clemens, S., An, Z., and Zhiwei, Y.: Astronomical timescale and palaeoclimatic implication of stcked 3.6 Myr monsoon records from the Chinese Loess Plateau, Quaternary Sci. Rev., 25, 33–48, 2006.
Tachikawa, K., Sépulcre, S., Toyofuku, T., and Bard, E.: Assessing influence of diagenetic carbonate dissolution on planktonic foraminiferal Mg/Ca in the southeastern Arabian Sea over the past 450 ka: Comparison between *Globigerinoides ruber* and *Globigerinoides sacculifer*, Geochem. Geophys. Geosyst., 9, Q04037, doi:10.1029/2007GC001904, 2008.
Tjallingii, R., Rohl, U., Kolling, M., and Bickert, T.: Influence of the water content on X-ray fluorescence core-scanning measurements in soft marine sediments, Geochem. Geophys. Geosyst., 8, Q02004, doi:10.1029/2006GC001393, 2007.
Wang, P., Clemens, S., Beaufort, L., Braconnot, P., Ganssen, G., Jian, Z., Kershaw, P., and Sarnthein, M.: Evolution and variability of the Asian monsoon system: State of the art and outstanding issues, Quaternary Sci. Rev., 24(5–6), 595–629, 2005.
Wang, P., Tian, J., Cheng, X., Liu, X., and Xu, J.: Carbon reservoir changes preceded major ice-sheet expansion at the mid-Brunhes event, Geology, 31(3), 239–242, 2003.
Wang, Y., Cheng, H., Edwards, R. L., He, Y., Kong, X., An, Z., Wu, J., Kelly, M. J., Dykoski,

C. A., and Li, X.: The Holocene Asian monsoon: Links to solar changes and North Atlantic climate, Science, 308, 854–857, 2005.
Wang, Y., Cheng, H., Edwards, R. L., Kong, X., Xiaohua, S., Chen, S., Wu, J., Jiang, X., Wang, X., and Zhisheng, A.: Millenial- and orbital-scale changes in the East Asian monsoon over the past 224 000 years, Nature, 28, 1090–1093, 2008.
Wang, Y. J., Cheng, H., Edwards, R. L., An, Z. S., Wu, J. Y., Shen, C. C., and Dorale, J. A.: A high-resolution absolute-dated late Pleistocene monsoon record from Hulu Cave, China, Science, 294, 2345–2348, 2001.
Wiewiora, A., Giresse, P., Petit, S., and Wilamowski, A.: A deep-water glauconitization process on the ivory coast-Ghana marginal ridge (ODP site 959): Determination of Fe^{3}+-rich Montmorillonite in Green Grains, Clay. Clay Miner., 49(6), 540–558, 2001.
Qiuzhen, Y., Berger, A., Driesschaert, E., Goosse, H., Loutre, M. F., and Crucifix, M.: The Eurasian ice sheet reinforces the East Asian summer monsoon during the interglacial 500 000 years ago, Clim. Past, 4, 79–90, 2008, http://www.clim-past.net/4/79/2008/.
Yin, Q. Z. and Guo, Z. T.: Strong summer monsoon during the cool MIS-13, Clim. Past, 4, 29–34, 2008, http://www.clim-past.net/4/29/2008/.
Ziegler, M., Lourens, L. J., Tuenter, E., Hilgen, F. J., Reichart, G. J., and Weber, S. L.: Decoupled precession phase of the Indian summer monsoon and productivity in the Arabian Sea, Paleoceanography, in review, 2009.
Ziegler, M., Jilbert, T., De Lange, G. J., Lourens, L. J., and Reichart, G.-J.: Bromine counts from XRF scanning as an estimate of the marine organic carbon content of sediment cores, Geochem. Geophys. Geosyst., 9, Q05009, doi:10.1029/2007GC001932, 2008.

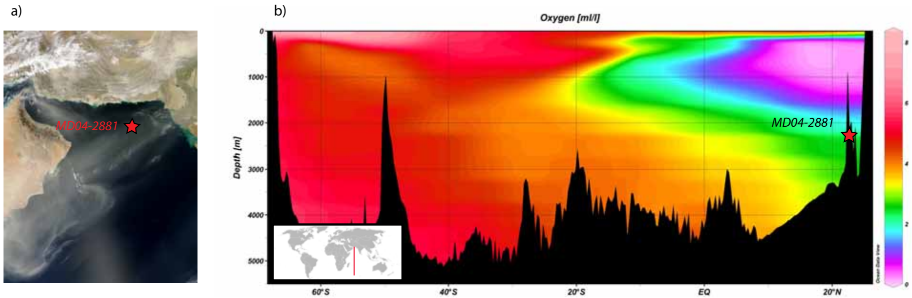

Fig. 1. **(a)** NASA's Aqua satellite picture, using the Moderate Resolution Imaging Spectroradiometer (MODIS) on 3 March 2009 (http://earthobservatory.nasa.gov/NaturalHazards). Star indicates position of IMAGES Core MD04-2881 was recovered on 14 October 2004, from a water depth of 2387 m at the Murray Ridge (22°12′5″ N–63°5′5″ E) in the northeastern Arabian Sea **(b)** oxygen profile through the Northern Arabian Sea.

CPD

5, 1989–2018, 2009

Anomalously high Arabian Sea productivity conditions

M. Ziegler et al.

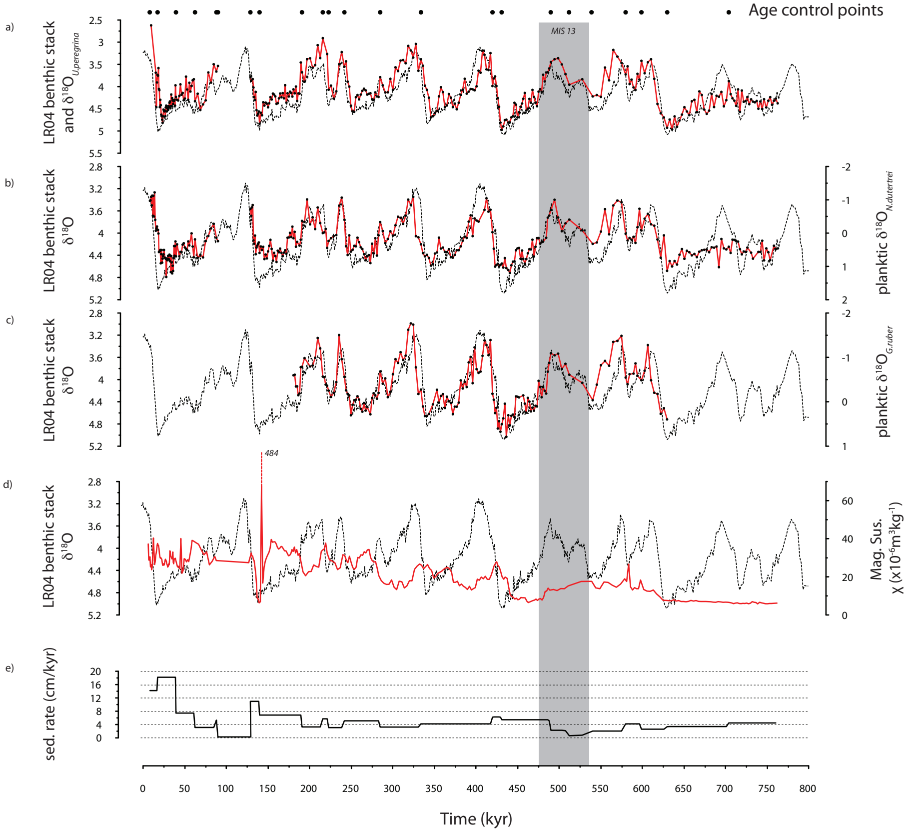

Fig. 2. Stable isotope records from MD04-2881 versus the global benthic isotope stack LR04 (black stippled line) (Lisiecki and Raymo, 2005). **(a)** Benthic δ^{18}O (*Uvigerina perigrina*); **(b)** planktic δ^{18}O of *Neoglobigerina dutertrei*; **(c)** planktic δ^{18}O of *Globigerinoides ruber*; **(d)** magnetic susceptibility; **(e)** sedimentation rates of MD04-2881.

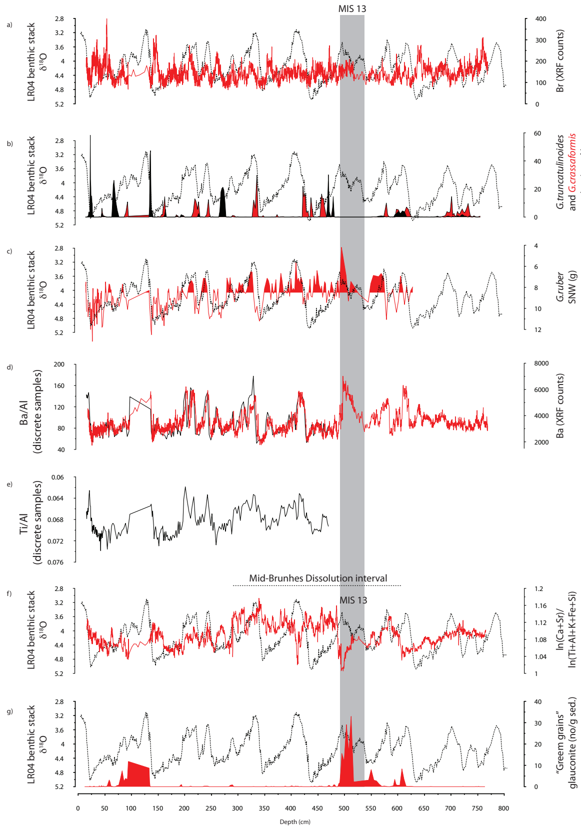

Fig. 3. Proxy records from MD04-2881 versus the global benthic isotope stack LR04 (black stippled line) (Lisiecki and Raymo, 2005). **(a)** Bromine counts (XRF-core scanning); **(b)** occurrence of *Globorotalia truncatulinoides* and *Globorotalia crassaformis*; **(c)** Ba/Al (black line; XRF measurements on discrete samples) and Ba counts (red line; XRF-core scanning); **(d)** size normalized weights of *G. ruber*; **(e)** Ti/Al (XRF measurements on discrete samples); **(f)** Ca+Sr over terrestrial elements (XRF-core scanning); **(g)** green grains (no/g sediment).

CPD

5, 1989–2018, 2009

Anomalously high Arabian Sea productivity conditions

M. Ziegler et al.

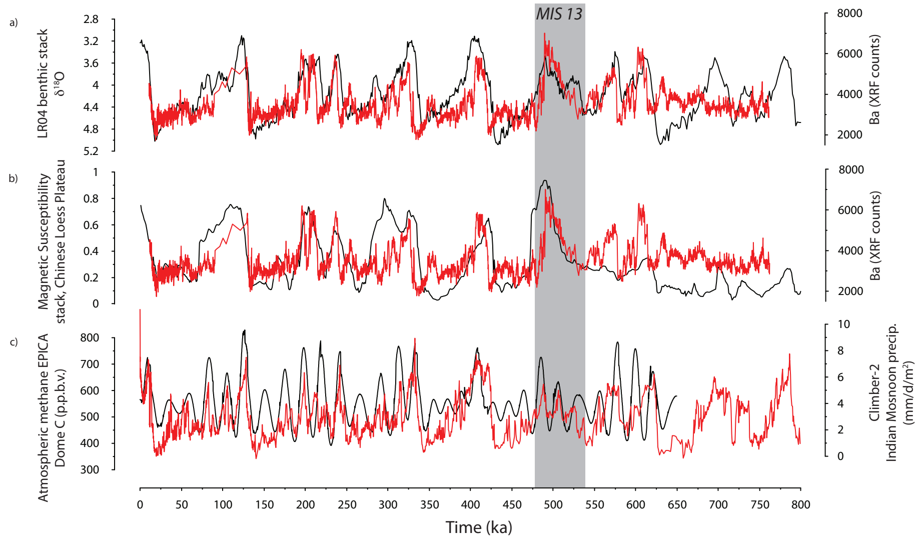

Fig. 4. Comparison between the Ba record of MD04-2881 and other paleoclimate-records. **(a)** Comparison with LR04 benthic isotope stack; **(b)** comparison with magnetic susceptibility stack from the Chinese Loess Plateau (Clemens et al., 2008); **(c)** atmospheric methane concentration from EPICA Dome C (Loulergue et al., 2008) compared with modeled Indian monsoon precipitation (CLIMBER-2) (Ziegler, et al., 2009).

CPD
5, 1989–2018, 2009